Tetrahedron model for the optical dielectric function of hydrogenated amorphous silicon nitride alloys

Z. Yin and F. W. Smith
Department of Physics, City College of the City University of New York, New York, New York 10031
(Received 27 December 1989)

A microstructural model based on Si-centered tetrahedra is proposed for hydrogenated amorphous silicon nitride (a-$Si_xN_yH_z$) alloys. The dependence of the optical dielectric function $\epsilon=\epsilon_1+i\epsilon_2$ of the a-$Si_xN_yH_z$ alloys on stoichiometry ([N]/[Si] ratio) and hydrogen content has been determined for (1) Si-rich a-Si_xN_{1-x} alloys (containing no hydrogen), using five tetrahedra, Si—$Si_{4-i}N_i$ ($i=0$–4) and (2) N-rich a-$Si_xN_{y-z}(NH)_z$ alloys, again using five tetrahedra, Si—$N_{4-i}(NH)_i$ ($i=0$–4). Specific alloys of interest for which ϵ has been predicted using the Bruggemann effective-medium approximation include a-Si_3N_4 and a-$Si(NH)_2$, amorphous silicon diimide. The predictions of the model for ϵ, the optical energy gap E_{opt}, and the index of refraction n have been obtained considering both random bonding and phase separation in the alloys. These predictions are compared here with previous experimental results, while a more comprehensive comparison with experiment for some N-rich a-$Si_xN_yH_z$ films is presented in the following paper.

I. INTRODUCTION

Amorphous Si-based alloys are of great current interest not only due to their important applications but also as widely studied examples of primarily tetrahedrally coordinated amorphous semiconductors. Studies of the optical response of such alloy films have provided a wealth of information concerning the microstructure, i.e., local atomic bonding configurations, present in the films.[1–3] In this paper a microstructural model based on a random mixture of Si-centered tetrahedra will be presented and developed for hydrogenated amorphous silicon nitride (a-$Si_xN_yH_z$) alloys. The predictions of the model for the optical dielectric function $\epsilon=\epsilon_1+i\epsilon_2$ will be compared with experimental results for a-$Si_xN_yH_z$ alloy films, both in this paper and also in paper II (Ref. 4) where the results of a careful study of the optical dielectric function, infrared absorption, and density of some N-rich films are presented. The goal of this research is to obtain as clear a correlation as possible between the microstructure and the macroscopic optical response of these films.

In the Si-centered tetrahedron model, the tetrahedra are considered to be the fundamental structural units determining the optical response of the alloys. This approach was first introduced by Philipp[2,5] for amorphous silicon-oxygen-nitrogen alloys and was further developed by Aspnes and Theeten,[6] who correctly combined it with the Bruggemann effective-medium approximation (EMA).[7] Si-centered tetrahedra have also been employed as the natural structural units for determining the Si—H bond-stretching frequencies[8,9] in amorphous Si alloys, the Si—O and Si—N bond-stretching frequencies in a-$Si_xO_yN_z$ alloys,[10] and the Si $2p$ core-level binding energies in a-$Si_xN_yH_z$ alloys.[11,12] In addition, the tetrahedron model has already been applied to a-$Si_xC_yH_z$ (Ref. 13) and a-Si:H (Ref. 14) alloys for the determination of the optical dielectric function. A previous application of this model to the optical response of a-Si:H/a-$Si_xN_yH_z$ multilayers has also been presented.[15]

One important new feature of the present work is the explicit incorporation of hydrogen atoms in the Si-centered tetrahedra. In this way it has been possible to study separately the effects on the optical response of varying the alloy stoichiometry, i.e., the [N]/[Si] ratio, and of varying the H content of the alloys. In addition, the model has now been extended to include nitrogen rich alloys ([N]/[Si] $>\frac{4}{3}$). In particular, predictions have been made for the optical response of amorphous silicon diimide, a-$Si(NH)_2$, a compound whose significance for the study of a-$Si_xN_yH_z$ alloys has been stressed by Tsu *et al.*[16]

The tetrahedron model will be presented in Sec. II, with the predictions of the model for ϵ_1,ϵ_2, the optical energy gap E_{opt}, and the static index of refraction n following in Sec. III. Comparisons with some previous studies of a-$Si_xN_yH_z$ films will also be presented in Sec. III. Our own experimental results for ϵ_1 and ϵ_2 for some N-rich films will be presented and compared with the predictions of the tetrahedron model in Paper II.[4]

II. TETRAHEDRON MODEL DEVELOPMENT

The goal of the Si-centered tetrahedron model as developed here is to provide an appropriate and convenient framework for calculating ϵ_1 and ϵ_2 for the a-$Si_xN_yH_z$ alloys under consideration. Using the model it will be possible to explore the effects of varying the alloy stoichiometry and hydrogen content on the optical response of the alloys. In order to accomplish this, the tetrahedron probabilities P_i will first be derived as functions of the alloy composition. The ϵ_i for the tetrahedra will then be obtained using the scaling procedure developed first by Aspnes and Theeten.[6] In Sec. III, the P_i and ϵ_i will be incorporated into the Bruggemann EMA

(Ref. 7) in order to obtain predictions for the optical dielectric functions of the a-$Si_xN_yH_z$ alloy films of interest. The photon energy range considered here extends from the near infrared through the visible up to the near-ultraviolet region (10 eV).

It is appropriate from the outset to impose some restrictions on the local atomic bonding configurations to be considered for these a-$Si_xN_yH_z$ alloys. In particular, H—H and N-H_3 configurations, i.e., H_2 and NH_3 molecules, are excluded since these units would not be part of the network. Also, N—N single bonds (1.7 eV) are excluded from consideration as Si—N (3.5 eV) and N—H (4.1 eV) bonds are much more stable.[17] There may also be steric limitations on the existence of N—N bonds in these alloys. Although the approach[2,5] followed here is generally referred to as the "random-bonding model" (RBM), in fact the bonding in the tetrahedra is not completely random. Since the number of possible Si—N bonds is maximized in the RBM, the alloys considered actually possess considerable short-range chemical ordering. In addition, the issue of whether the bonds are homogeneously dispersed throughout the alloy, as assumed by the RBM, or phase separated into distinct regions is an important one and will be discussed below.

Each Si atom at the center of a tetrahedron has four valence electrons available, each of which can participate in a bond to one of the following five bonding units: Si(4), H(1), N(3), NH(2), and NH_2(1). The number of valence electrons which each of these units has available for bonding to the network is indicated in parentheses. By distinguishing between the N, NH, and NH_2 bonding units, some potentially important second-nearest-neighbor effects are included in the model. The contribution of Si dangling bonds to the optical dielectric function is not included in this model since observed spin densities (less than 10^{19} cm^{-3} in hydrogenated and 10^{20} cm^{-3} in hydrogen-free silicon nitride[12]) are small compared to typical Si-atom concentrations[4] of $(2-3)\times10^{22}$ cm^{-3}. The number of distinct Si-centered tetrahedra which can be constructed from these bonding units is given by $N=(n+k-1)!/[k!(n-1)!]$, where $n=5$ is the number of distinct bonding units and $k=4$ is the number of valence electrons which the central Si has available for bonding. There are thus $N=8!/(4!4!)=70$ possible tetrahedra for a-$Si_xN_yH_z$ alloys. To include all 70 tetrahedra would make the model too complicated to be useful. The model will therefore focus only on some special cases which are reasonably simple yet meaningful enough to correspond to physically attainable alloy films.

Another potentially useful approach to bonding in a-$Si_xN_yH_z$ alloys is to consider N-centered units, of which there are only three possibilities: N-Si_3, N-Si_2H, and N-SiH_2. It is not possible, however, to develop a model for the optical response of the alloys based only on these three units as Si—Si bonds which absorb strongly in the photon energy range of interest are not explicitly included.

A. a-Si_xN_{1-x} ($\frac{3}{7}<x<1$)

Hydrogen-free a-Si_xN_{1-x} alloys containing only Si—Si and Si—N bonds will be considered first. These include the Si-rich alloys for which the [N]/[Si] ratio $(1-x)/x$ is less than the stoichiometric value of $\frac{4}{3}$. Since only Si and N are available for bonding to the central Si atom, the number of distinct tetrahedra is $N=5!/(4!1!)=5$, corresponding to Si-$Si_{4-i}N_i$, with $i=0-4$. This case has already been considered in detail by Aspnes and Theeten,[6] and so the presentation here will be brief. The probabilities P_i for these five tetrahedra can be expressed as functions of the composition parameter $x=f(\mathrm{Si})$, the fraction of Si atoms, with $1-x=f(\mathrm{N})$ being the fraction of N atoms. In accord with the RBM, homogeneous dispersion of the Si—Si and Si—N bonds throughout the alloy will be assumed, while phase separation into separate regions corresponding to a-Si and a-Si_3N_4 will be treated as a special case.

The fraction of Si atoms in the alloy which can bond to a given Si atom is given by

$$f_1(\mathrm{Si})=f(\mathrm{Si})-3f(\mathrm{N})/4=x-3(1-x)/4=(7x-3)/4\ , \tag{1}$$

which is less than $f(\mathrm{Si})$ by the amount $3f(\mathrm{N})/4$ which is equal to the fraction of Si atoms required to satisfy the bonds of all the N atoms present. Thus, these Si atoms are effectively unavailable to bond to other Si atoms. Note that $f_1(\mathrm{N})=1-x$ since N atoms are bonded only to Si atoms. Finally, the fractions of all atoms which can bond to a Si atom which are Si or N atoms are given by

$$f_2(\mathrm{Si})=4f_1(\mathrm{Si})/[4f_1(\mathrm{Si})+3f_1(\mathrm{N})]=(7x-3)/4x \tag{2}$$

and

$$f_2(\mathrm{N})=3f_1(\mathrm{N})/[4f_1(\mathrm{Si})+3f_1(\mathrm{N})]=3(1-x)/4x\ ,$$

respectively, where the fact that Si has four valence electrons while N has three valence electrons available for bonding has been explicitly included. The $P_i(x)$ for the five Si-$Si_{4-i}N_i$ ($i=0-4$) tetrahedra under consideration are given in the RBM by

$$P_i=\frac{4!f_2^{4-i}(\mathrm{Si})f_2^i(\mathrm{N})}{(4-i)!i!}\ , \tag{3}$$

and are shown in the left-hand side of Fig. 1 as functions of the [N]/[Si] ratio $y/x=(1-x)/x$ from $y/x=0$ to $\frac{4}{3}$. The $P_i(x)$ are also given in Table I, along with the volumes V_i associated with each tetrahedron. Note that these $P_i(x)$ are not valid for $y/x>\frac{4}{3}$, the [N]/[Si] ratio above which N—N bonds would have to be present in these hydrogen-free films. If the Si—Si and Si—N bonds are phase separated into regions containing only Si-Si_4 or Si-N_4 tetrahedra, i.e., a-Si or a-Si_3N_4, then the corresponding tetrahedron probabilities are given by $P_1=f_2(\mathrm{Si})$, $P_2=P_3=P_4=0$, and $P_5=f_2(\mathrm{N})$.

Since the ϵ_i for the five tetrahedra are, in general, not available from experiment, the scaling approach of Aspnes and Theeten[6] will be used to obtain the ϵ_i by scaling from the measured ϵ of a-Si. This approach is based on the dielectric model of Phillips,[18] van Vechten,[19] and Levine[20] and has been discussed in detail previously.[6,13,14] The results of the scaling are presented in Table I,

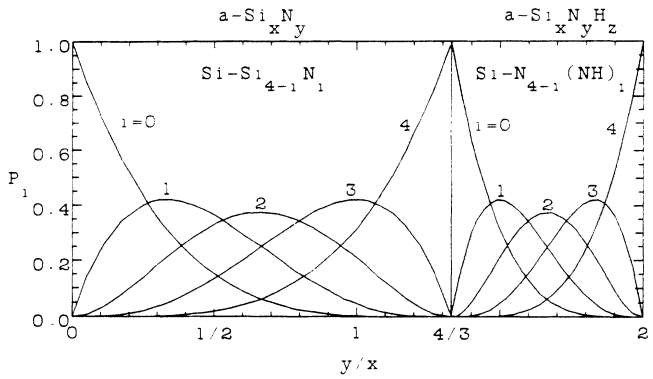

FIG. 1. Probabilities P_i for Si-centered tetrahedra as functions of [N]/[Si] ratio y/x. Left-hand side of figure: Si-$Si_{4-i}N_i$ ($i=0$–4) tetrahedra in a-Si_xN_{1-x} alloys for $0 \le y/x = (1-x)/x \le \frac{4}{3}$. Right-hand side of figure: Si-$N_{4-i}(NH)_i$ ($i=0$–4) tetrahedra in a-$Si_xN_{y-z}(NH)_z$ alloys for $\frac{4}{3} \le y/x \le 2$. [Note that $x+y+z=1$ and $z=(3r-4)/(4r-3)$ where $r=y/x$.]

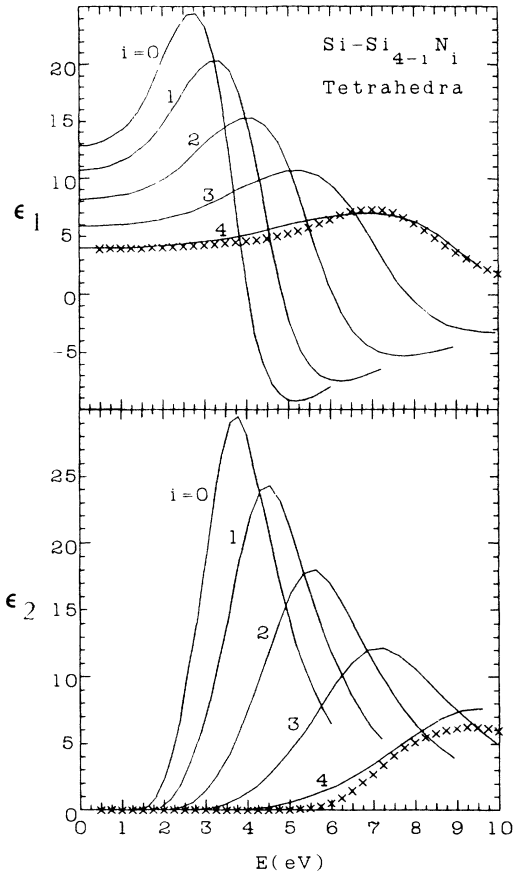

FIG. 2. Real part ϵ_1 and imaginary part ϵ_2 of the dielectric function vs energy E for Si-centered tetrahedra Si-$Si_{4-i}N_i$ ($i=0$–4), obtained by scaling from a-Si (see text). The experimental data of H. R. Philipp (Ref. 2) for a-Si_3N_4 (×) are included for comparison with the predictions for the $i=4$ tetrahedron Si-N_4.

where $\langle r \rangle = (4-i)r(\text{Si—Si})/4 + ir(\text{Si—N})/4$, with $r(\text{Si—Si}) = 1.176$ Å and $r(\text{Si—N}) = 0.867$ Å. E_H and C are the homopolar and heteropolar parts of E_g, the average-energy-gap parameter. The energy scaling parameter C_2 and the parameter C_1 which scales the magnitude of ϵ are also given in Table I for the five tetrahedra.

We note that the lone-pair electrons associated with the N atoms have not been included here in the dielectric model even though they have been predicted to lie near the top of the valence band for stoichiometric films and thus might be expected to contribute to the optical response. Aspnes and Theeten[6] have attempted to indirectly include the lone-pair electrons in the model by using the measured ϵ of a-Si_3N_4 for the contribution of the Si—N bonds. Martin-Moreno *et al.*[21] have pointed out, however, that the lone-pair contribution to the optical response can be neglected to a large degree due to a low cross-section for transitions from the lone-pair states to the states lying at the bottom of the conduction band, which are spatially separated from them.

In Fig. 2 the scaling predictions for ϵ_1 and ϵ_2 for the five tetrahedra are given as functions of photon energy E. The curves for $i=0$ correspond to the data of Aspnes *et al.*[22] for hydrogen-free chemical-vapor-deposited (CVD) a-Si. It is apparent that the maxima in both ϵ_1 and ϵ_2 decrease in magnitude and shift to higher energies as stronger Si—N bonds replace weaker Si—Si bonds, as expected. In previous work[15] the ϵ_1 and ϵ_2 spectra for these tetrahedra were scaled from a-Si:H in order to at least partially account for the effects of hydrogen bonded

TABLE I. Tetrahedron probabilities P_i, volumes V_i, and scaling parameters for a-Si_xN_{1-x} alloys.

Tetrahedron	i	P_i[a]	V_i (Å^3)	$\langle r \rangle$ (Å)	E_H (eV)	C (eV)	E_g[b] (eV)	C_1[c]	C_2[d]
Si-Si_4	0	$f_2^4(\text{Si})$	20.02	1.176	4.76	0	4.76	1.00	1.00
Si-Si_3N	1	$4f_2^3(\text{Si})f_2(\text{N})$	21.08	1.099	5.64	0.94	5.72	0.824	0.832
Si-Si_2N_2	2	$6f_2^2(\text{Si})f_2^2(\text{N})$	22.13	1.022	6.75	2.16	7.09	0.610	0.671
Si-SiN_3	3	$4f_2(\text{Si})f_2^3(\text{N})$	23.18	0.944	8.22	3.91	9.10	0.413	0.523
Si-N_4	4	$f_2^4(\text{N})$	24.24	0.867	10.15	6.50	12.05	0.257	0.395

[a] $f_2(\text{Si}) = (7x-3)/4x$ and $f_2(\text{N}) = 3(1-x)/4x$.
[b] $E_g^2 = E_H^2 + C^2$.
[c] $C_1 = [n(i)/n(i=0)]C_2^2$, where n is the density of bonding electrons.
[d] $C_2 = E_g(i=0)/E_g(i)$.

in the alloys. Since the effects of hydrogen will be explicitly included below, it is more appropriate now to scale from a-Si. The spectra shown for the $i=4$ tetrahedron, Si-N_4, correspond to a-Si_3N_4. The measured spectra obtained by Philipp[2] for CVD a-Si_3N_4 are shown for comparison.

B. a-$Si_xN_yH_z$

The incorporation of hydrogen in the alloys will now be explicitly considered by including the bonding of H in the Si-centered tetrahedra. Two cases will be considered, the first corresponding to N-rich ($[N]/[Si]>\frac{4}{3}$) alloy films which are typically prepared via plasma-enhanced CVD using high $[NH_3]/[SiH_4]$ ratios R. For R high enough ($R>20$), the films can be shown to essentially contain only Si—N and N—H bonds,[4] so that Si—H and Si—Si bonds can be ignored to a first approximation. The second case will include Si—H and Si—Si bonds and thus is more appropriate for films prepared using lower values of R.

1. a-$Si_xN_yH_z=a$-$Si_xN_{y-z}(NH)_z$

There are now only Si—N and N—H bonds present in the alloys and, in addition, only two units will be allowed to bond to the central Si, namely, N and NH. NH_2 bonding units are not included at this stage, primarily because little evidence has been found for their existence in the films studied.[4] The number of distinct tetrahedra is again five, given by Si-$N_{4-i}(NH)_i$ with $i=0$–4. Note that the $i=4$ or Si-$(NH)_4$ tetrahedron corresponds to silicon diimide $Si(NH)_2$,

Using the same notation as in Sec. II A, it follows that

$$f_1(\mathrm{Si})=x-\tfrac{3}{4}(y-z)-\tfrac{2}{4}z=\tfrac{1}{4}(4x-3y+z)=0\ ,$$

$$f_1(\mathrm{N})=y-z\ ,$$

and (4)

$$f_1(\mathrm{NH})=z\ ,$$

where the fact that each NH unit can bond to only two tetrahedra has been taken into account. Note that $f_1(\mathrm{Si})=0$ due the absence of Si—Si bonds and that this yields the supplemental condition $4x-3y+z=0$. Finally, we have that

$$f_2(\mathrm{Si})=0\ ,$$

$$f_2(\mathrm{N})=3(y-z)/4x\ ,$$

and (5)

$$f_2(\mathrm{NH})=z/2x\ .$$

The tetrahedron probabilities P_i are given in the random-bonding model by

$$P_i=\frac{4!f_2^{4-i}(\mathrm{N})f_2^{i}(\mathrm{NH})}{(4-i)!i!} \tag{6}$$

and thus have the same functional form as those given previously in Eq. (3).

The P_i for these tetrahedra are shown on the right-hand side of Fig. 1 as functions of the [N]/[Si] ratio y/x ($\frac{4}{3}\le y/x\le 2$) and are also presented in Table II, along with the tetrahedron volumes and scaling parameters C_1 and C_2. In the dielectric model it has been assumed that $r(\mathrm{Si—N})=r(\mathrm{Si—NH})$ and that nitrogen lone-pair electrons can again be omitted. The volume $V_0=27.25$ Å^3 for Si-N_4 has been obtained by using a density[23] of 2.86 g/cm^3 for a-Si_3N_4. For Si-$(NH)_4$, i.e., $Si(NH)_2$, an analysis carried out in paper II (Ref. 4) for a N-rich film with a measured density of 2.08 g/cm^3 has yielded $V_4=48.81$ Å^3. This analysis has made use of ir absorption results to obtain experimental values for the P_i for this film. It should be noted that this tetrahedron volume V_4 corresponds to a density of 1.98 g/cm^3 for a-$Si(NH)_2$.

ϵ_1 and ϵ_2 for these tetrahedra have been scaled from the measured ϵ of Philipp[2] for a-Si_3N_4, with the results presented in Fig. 3. The spectra shown for $i=4$ correspond to the predictions of the model for a-$Si(NH)_2$. The gradual shifts of the maxima in both ϵ_1 and ϵ_2 to higher energies reflect increases in E_g and the average Si—N bond energy as the Si—N bond becomes more ionic. This prediction is in agreement with that of Robertson[24] who found an energy gap in the density of states for the Si—N_3(NH) tetrahedron (equivalent to his Si_2N_3H case) which was larger than that of Si—N_4.

TABLE II. Tetrahedron probabilities P_i, volumes V_i, and scaling parameters for a-$Si_xN_{y-z}(NH)_z$ alloys.

Tetrahedron	P_i[a]	V_i (Å^3)	E_H (eV)	C (eV)	E_g (eV)	C_1	C_2
Si-N_4	$f_2^4(\mathrm{N})$	27.25	10.15	6.75	12.19	1.00	1.00
Si-N_3(NH)	$4f_2^3(\mathrm{N})f_2(\mathrm{NH})$	32.64	10.15	7.87	12.84	0.846	0.949
Si-$N_2(NH)_2$	$6f_2^2(\mathrm{N})f_2^2(\mathrm{NH})$	38.03	10.15	8.69	13.36	0.745	0.912
Si-N$(NH)_3$	$4f_2(\mathrm{N})f_2^3(\mathrm{NH})$	43.42	10.15	9.29	13.76	0.677	0.886
Si-$(NH)_4$	$f_2^4(\mathrm{NH})$	48.81	10.15	9.71	14.05	0.630	0.867

[a] $f_2(\mathrm{N})=3(y-z)/4x$ and $f_2(\mathrm{NH})=z/2x$.

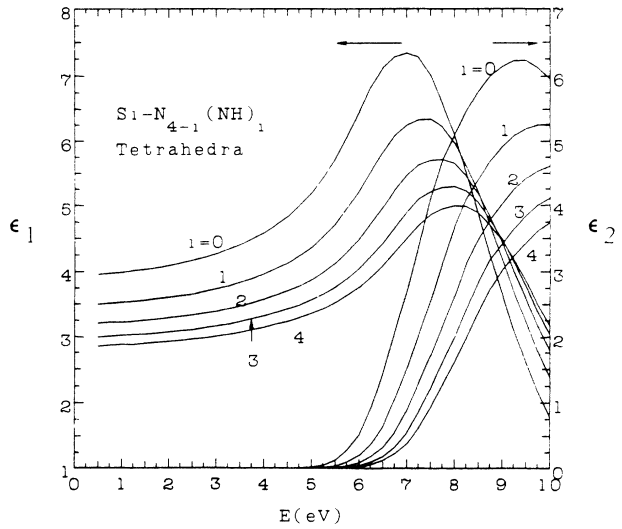

FIG. 3. Real part ϵ_1 and imaginary part ϵ_2 of the dielectric function vs energy E for Si-centered tetrahedra Si-$N_{4-i}(NH)_i$ ($i=0$–4), obtained by scaling from a-Si_3N_4 (see text).

2. *Tetrahedra containing Si—H or Si—Si bonds*

For a-$Si_xN_yH_z$ films prepared using low $[NH_3]/[SiH_4]$ ratios ($R \leq 20$), experiments[4] indicate that Si—H and Si—Si bonds will be present in the films in addition to Si—N and N—H bonds. Tetrahedron volumes and scaling parameters are listed in Table III for the six tetrahedra which have been used in Paper II (Ref. 4) in EMA fits to the measured ϵ_1 and ϵ_2 for the films studied. These tetrahedra include two containing Si—H bonds [Si-$HN(NH)_2$ and Si-$HN_2(NH)$] and four containing Si—Si bonds [Si-$Si(NH)_3$, Si-$SiN(NH)_2$, Si-$SiN_2(NH)$, and Si-Si_2N_2]. The ϵ spectra for these tetrahedra, again obtained by scaling from Philipp's data[2] for a-Si_3N_4, are shown in Fig. 4. Note that the ϵ_1 and ϵ_2 spectra for tetrahedra containing 0, 1, or 2 Si—Si bonds are quite distinct from each other.

III. TETRAHEDRON MODEL PREDICTIONS

In addition to the predictions of the tetrahedron model for the ϵ_1 and ϵ_2 spectra of individual tetrahedra which have already been presented in Figs. 2, 3, and 4, predictions for specific a-$Si_xN_yH_z$ alloys can be obtained by using the EMA to determine the optical response of mixtures of tetrahedra. The Bruggemann EMA (Ref. 7) for the dielectric function ϵ of the alloy is given by

$$\sum_i v_i \frac{\epsilon_i - \epsilon}{\epsilon_i + 2\epsilon} = 0 , \qquad \sum_i v_i = 1 , \tag{7}$$

where v_i and ϵ_i are the volume fraction and dielectric

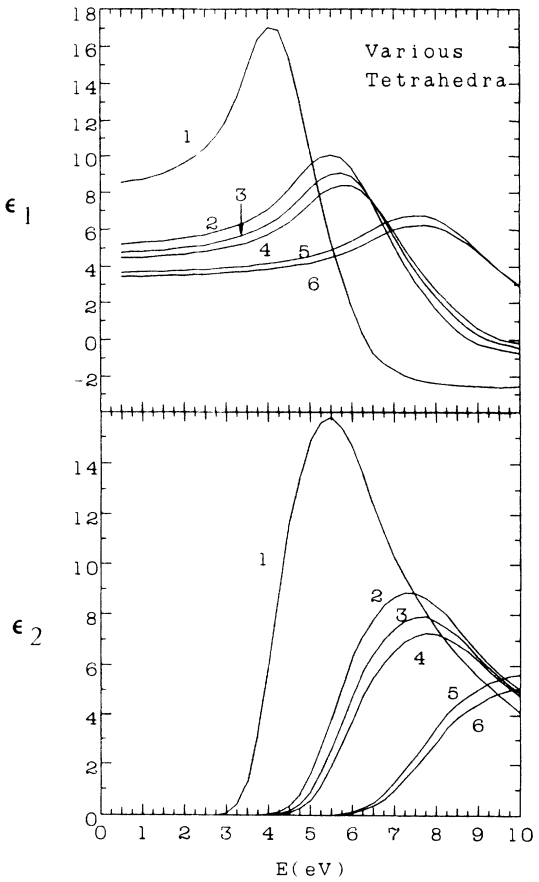

FIG. 4. Real part ϵ_1 and imaginary part ϵ_2 of the dielectric function vs energy E for six Si-centered tetrahedra, numbered as follows: (1) Si-Si_2N_2; (2) Si-$SiN_2(NH)$; (3) Si-$SiN(NH)_2$; (4) Si-$Si(NH)_3$; (5) Si-$HN_2(NH)$; (6) Si-$HN(NH)_2$.

TABLE III. Tetrahedron volumes V_i and scaling parameters for several Si-centered tetrahedra.

Tetrahedron	V_i (Å^3)	$\langle r \rangle$ (Å)	E_H (eV)	C (eV)	E_g (eV)	C_1[a]	C_2[a]
Si-$HN(NH)_2$	34.34	0.835	11.13	7.38	13.36	0.826	0.912
Si-$HN_2(NH)$	28.95	0.835	11.13	7.01	13.16	0.908	0.926
Si-$Si(NH)_3$	41.61	0.944	8.21	6.03	10.19	1.171	1.196
Si-$SiN(NH)_2$	36.22	0.944	8.21	5.59	9.93	1.274	1.227
Si-$SiN_2(NH)$	30.83	0.944	8.21	4.95	9.59	1.428	1.271
Si-Si_2N_2	23.64	1.022	6.76	2.22	7.11	2.539	1.714

[a]Note that $C_1 = C_2 = 1$ corresponds to Si-N_4.

function, respectively, of the ith component, taken here to be the Si-centered tetrahedra. Given an alloy of composition x,y,z, the $v_i(x,y,z)$ to be used in the EMA are given in terms of the $P_i(x,y,z)$ and V_i by

$$v_i(x,y,z)=\frac{P_i(x,y,z)V_i}{\sum_i P_i(x,y,z)V_i} , \tag{8}$$

where the sum is over all the possible tetrahedra in the alloy. Using the ϵ_i for the tetrahedra given in Figs. 2, 3, and 4, the ϵ for the alloy of interest is obtained from Eq. (7). Results for specific alloys will now be presented.

A. a-Si_xN_{1-x} ($\frac{3}{7} \le x \le 1$)

The predicted ϵ_1 and ϵ_2 for several a-Si_xN_{1-x} alloys with x lying between 1 (a-Si) and $\frac{3}{7}$ (a-Si_3N_4) are presented in Fig. 5 for the case of random bonding, with the tetrahedron probabilities P_i given by Eq. (3). The spectra evolve smoothly as x decreases from 1 to $\frac{3}{7}$, reflecting the smooth evolution of the ϵ_i for the tetrahedra shown in Fig. 2. The agreement between the $i=4$ spectra and the measured spectra for a-Si_3N_4 of Philipp[2] as shown in Fig. 2 is quite good with regard to the shift of the energy scale, given by C_2. The agreement for the magnitude of ϵ_1 is also good, while the measured ϵ_2 lies somewhat below the prediction of the model. The assumption of the model that the lone-pair electrons of the nitrogen atoms do not contribute significantly to the optical response of the alloys thus appears to be consistent with experiment.

The predicted variations of the optical energy gap $E_{\rm opt}$, defined by

$$\epsilon_2(E)=B(E-E_{\rm opt})^2/E^2 , \tag{9}$$

and the static index of refraction n are shown in Fig. 6 as functions of the [N]/[Si] ratio $(1-x)/x$ for the cases of random bonding and of phase separation. For both cases, n is predicted to decrease almost linearly with N/Si, in agreement with experiments on amorphous silicon nitride both with and without incorporated H.[25,26] The prediction that appreciable changes occur in n before they occur in $E_{\rm opt}$ is also consistent with experiment.[27]

$E_{\rm opt}$ is predicted for both cases to increase slowly initially and then much more rapidly as the stoichiometric [N]/[Si] ratio of $\frac{4}{3}$ is approached, in good agreement with other theoretical predictions.[21] This rapid increase in $E_{\rm opt}$ is a clear signal of the disappearance from the alloy of the more strongly absorbing Si—Si bonds, see Fig. 1, and is qualitatively consistent with experimental observations.[25,28] It is clear, however, that the predicted increase in $E_{\rm opt}$ is less rapid for the case of phase separation since in this case the presence of strongly absorbing Si-Si_4 tetrahedra in the alloys enhances the low-energy optical absorption. Fewer Si-Si_4 tetrahedra will be present if the random-bonding model is valid and so for this case $E_{\rm opt}$ increases more rapidly as the [N]/[Si] ratio increases. Experimental determinations of $E_{\rm opt}$ tend to lie between the two curves in Fig. 6, thus indicating that partial phase separation may be occurring under certain deposition conditions.

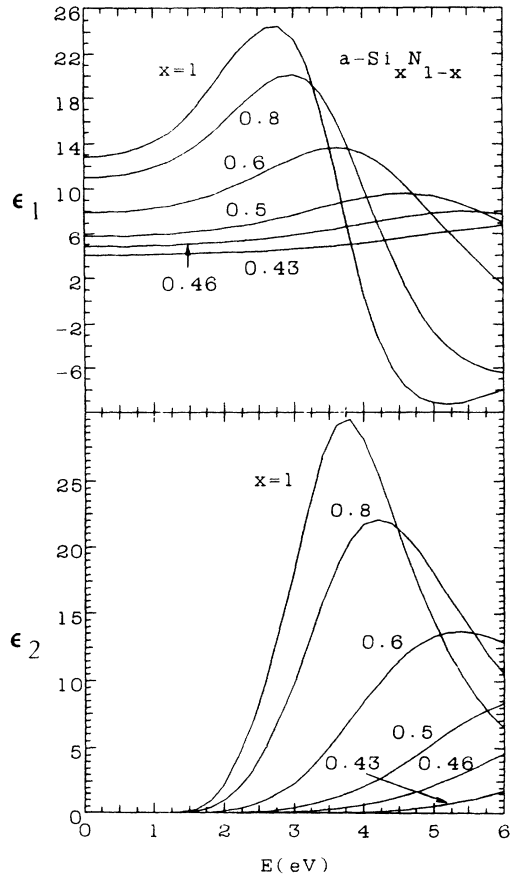

FIG. 5. Real part ϵ_1 and imaginary part ϵ_2 of the dielectric function vs energy E for a-Si_xN_{1-x} alloys, obtained using the EMA (see text). Curves are labeled with the Si fraction x.

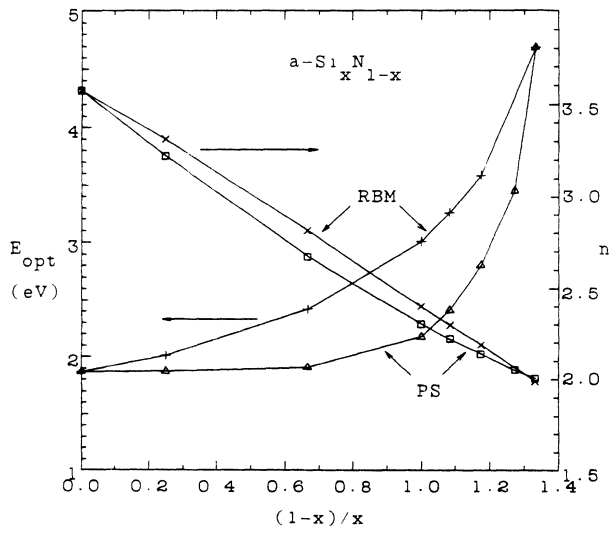

FIG. 6. Predicted optical energy gap $E_{\rm opt}$ and static index of refraction n vs [N]/[Si] ratio $(1-x)/x$ for a-Si_xN_{1-x} alloys. RBM (random-bonding model) corresponds to the case of homogeneous dispersion of the Si—Si and Si—N bonds, while PS corresponds to phase separation of the bonds.

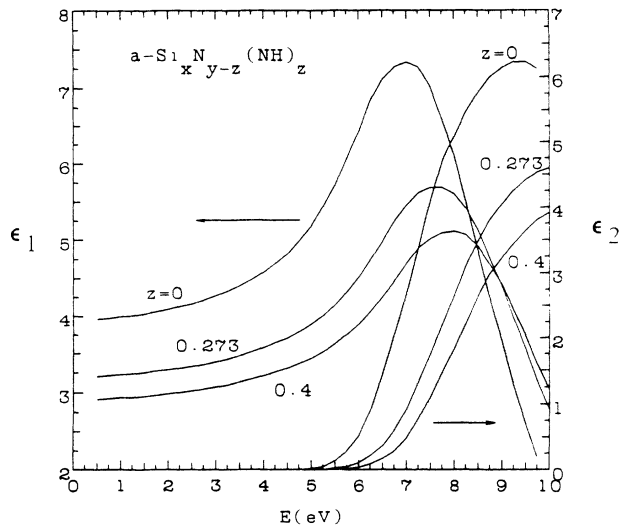

FIG. 7. Real part ϵ_1 and imaginary part ϵ_2 of the dielectric function vs energy E for a-$Si_xN_{y-z}(NH)_z$ alloys, obtained using the EMA (see text). Curves are labeled with the H fraction z, with $z=0$ corresponding to a-Si_3N_4, $z=0.273$ to a-$Si_3N_5H_3$, and $z=0.4$ to a-$Si(NH)_2$, amorphous silicon diimide. Note also that $x+y+z=1$, $4x-3y+z=0$, and $z=(3r-4)/(4r-3)$ where $r=y/x$ for these N-rich alloys.

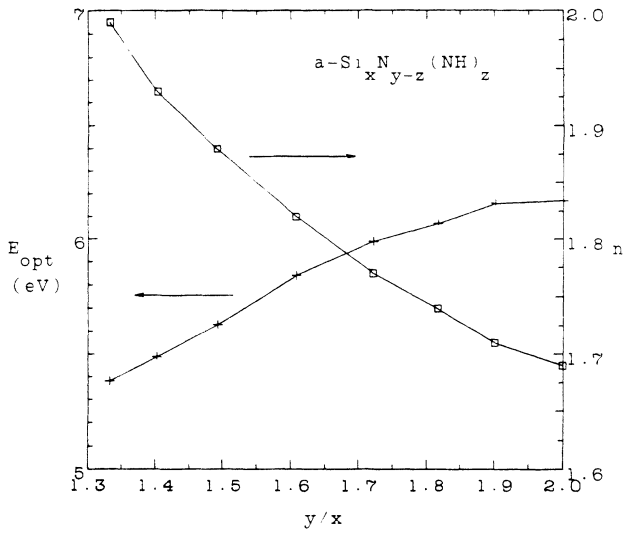

FIG. 8. Predicted optical energy gap E_{opt} and static index of refraction n vs [N]/[Si] ratio y/x for a-$Si_xN_{y-z}(NH)_z$ alloys. Note that $x+y+z=1$, $4x-3y+z=0$, and $z=(3r-4)/(4r-3)$ where $r=y/x$ for these N-rich alloys.

B. a-$Si_xN_{y-z}(NH)_z$

In Fig. 7 the predicted ϵ_1 and ϵ_2 spectra for three alloys are shown with N/Si$=y/x=\frac{4}{3}$, $\frac{5}{3}$, and 2, corresponding to hydrogen fractions of $z=0$, 0.273, and 0.4, respectively. Note that these three alloys contain, respectively, all Si—N bonds (a-Si_3N_4), half Si—N and half Si—NH bonds (a-$Si_3N_5H_3$), and all Si—NH bonds [a-$Si(NH)_2$]. The predicted values of E_{opt} for these specific alloys, shown in Fig. 8, are 5.38, 5.88, and 6.17 eV, reflecting an increase in C, the heteropolar or ionic part of E_g, as the number of NH bonding units in the alloy increases. At the same time, the predicted values of n, also shown in Fig. 8, decrease from 1.99 to 1.79, and finally to 1.69 for a-$Si(NH)_2$. Detailed comparisons with the measured ϵ_1 and ϵ_2 spectra of some N-rich a-$Si_xN_yH_z$ films are presented in paper II.[4]

IV. CONCLUSIONS

A microstructural model based on Si-centered tetrahedra has been proposed for a-$Si_xN_yH_z$ alloys which explicitly considers both the effects of stoichiometry and of hydrogen content on film properties. Alloys both with and without incorporated hydrogen have been considered, including a-Si_3N_4 and a-$Si(NH)_2$, amorphous silicon diimide. Predictions of the model for ϵ_1 and ϵ_2, the optical energy gap E_{opt}, and the static index of refraction n have been obtained and compared with previous experimental results. Good qualitative agreement with experiment has been found for the dependence of E_{opt} and n on composition and the issue of whether random bonding or phase separation occurs in these alloys has been discussed. Detailed comparisons with experimental results for some N-rich films are presented in paper II.

ACKNOWLEDGMENTS

We wish to thank Dr. K. Mui and Dr. D. V. Tsu for helpful discussions. This research has been supported by the U.S. Department of Energy under Grant No. DE-FG02-87ER45317.

[1]M. H. Brodsky, M. Cardona, and J. J. Cuomo, Phys. Rev. B **16**, 3556 (1977).
[2]H. R. Philipp, J. Electrochem. Soc. **120**, 295 (1973).
[3]K. Mui, D. K. Basa, F. W. Smith, and R. Corderman, Phys. Rev. B **35**, 8089 (1987); J. Non-Cryst. Solids **97/98**, 999 (1987).
[4]Z. Yin and F. W. Smith, the following paper, this issue, Phys. Rev. B **42**, 3666 (1990).
[5]H. R. Philipp, J. Phys. Chem. Solids **32**, 1935 (1971).
[6]D. E. Aspnes and J. B. Theeten, J. Appl. Phys. **50**, 4928 (1979).
[7]D. A. G. Bruggemann, Ann. Phys. (Leipzig) [Folge 5] **24**, 636 (1935).
[8]G. Lucovsky, Solid State Commun. **29**, 571 (1979).
[9]W. R. Knolle and J. W. Osenbach, J. Appl. Phys. **58**, 1248 (1985).
[10]T. S. Eriksson and C. G. Granqvist, J. Appl. Phys. **60**, 2081 (1986).
[11]R. Karcher, L. Ley, and R. L. Johnson, Phys. Rev. B **30**, 1896

(1984).
[12]S. Hasegawa, T. Tsukao, and P. C. Zalm, J. Appl. Phys. **61**, 2916 (1987); S. Hasegawa, M. Matuura, and Y. Kurate, Appl. Phys. Lett. **49**, 1272 (1986).
[13]K. Mui and F. W. Smith, Phys. Rev. B **35**, 8080 (1987).
[14]K. Mui and F. W. Smith, Phys. Rev. B **38**, 10 623 (1988).
[15]K. Mui and F. W. Smith, J. Non-Cryst. Solids **97/98**, 975 (1987); J. Appl. Phys. **63**, 475 (1988).
[16]D. V. Tsu, G. Lucovsky, and M. J. Mantini, Phys. Rev. B **33**, 7069 (1986).
[17]Single bond energies for N—N, Si—N, and N—H bonds have been obtained using the heats of formation $H_0(300\ \mathrm{K})$ of H, N, Si, NH_3, N_2H_4, and Si_3N_4 as given in the *JANAF Thermochemical Tables,* 2nd ed., edited by D. R. Stull and H. Prophet (U.S. GPO, Washington, D.C., 1971). See also the discussion in T. Makine and M. Maeda, Jpn. J. Appl. Phys. Pt. 1 **25**, 1300 (1986).
[18]J. C. Phillips, Phys. Rev. Lett. **20**, 550 (1968); Rev. Mod. Phys. **42**, 317 (1970).
[19]J. A. van Vechten, Phys. Rev. **182**, 891 (1969); **187**, 1007 (1969).
[20]B. F. Levine, J. Chem. Phys. **59**, 1463 (1973).
[21]L. Martin-Moreno, E. Martinez, J. A. Verges, and F. Yndurain, Phys. Rev. B **35**, 9683 (1987).
[22]D. E. Aspnes, A. A. Studna, and E. Kinsbron, Phys. Rev. B **29**, 768 (1984). These results obtained in the range from 1.5 to 6 eV have been extrapolated to 0 eV using the single oscillator expression [S.H. Wemple, J. Chem. Phys. **67**, 2151 (1977)].
[23]K. Niihara and T. Hirai, J. Mater. Sci. **11**, 604 (1976).
[24]J. Robertson, Philos. Mag. B **44**, 215 (1981).
[25]E. A. Davis, N. Piggins, and S. C. Bayliss, J. Phys. C **20**, 4415 (1987).
[26]W. A. P. Claassen, W. G. J. N. Valkenburg, F. H. P. M. Habraken, and Y. Tamminga, J. Electrochem. Soc. **130**, 2419 (1983).
[27]N. Ibaraki and H. Fritzsche, Phys. Rev. B **30**, 5791 (1984).
[28]C. Chaussat, E. Bustarret, J. C. Bruyere, and R. Groleau, Physica B+C (Amsterdam) **129B**, 215 (1985).